

Effects of TiC Additions on Physical Properties of W-2wt.%VC-1wt.%C Nano Powder Composites Fabricated by Mechanical Alloying

Sonmez S^{1,2*}, Jahangiri H¹ and Ovecoglu ML¹

¹Istanbul Technical University, Department of Metallurgical and Material Engineering, 34469, Istanbul, Turkey

²Hakkari University, Department of Mechanical Engineering, 30000, Hakkari, Turkey

Abstract

Effects of TiC additions on physical properties of W-VC-C nano powder composites during different milling time were investigated. W-2wt.%VC-1wt.%C and W-2wt.%VC-2wt.%TiC-1wt.%C composite powders were mechanically alloyed (MA'd) for 1 h, 3 h, 6 h, 12 h and 24 h in a high energy ball mill. Characterization studies were conducted to determine the effect of TiC content and MA duration on the morphology, lattice parameter, crystallite size and lattice strain amorphization rate of the powder composites. Addition of TiC declined particle size decreasing rate and powder densities after MA for 24 h. Both Gaussian and Williamson Hall (W-H) methods were employed on the X-ray diffraction patterns to analyse the variations of lattice strain and crystallite size with MA times. Up to MA durations of 6 h, the strain values increased rapidly and between MA times of 6 and 24 h, strain values enhancement occurred slowly in W-H method, while strain values obtained by Gaussian method increased linearly. The crystallite sizes of W-2wt.%VC-1wt.%C and W-2wt.%VC-2wt.%TiC-1wt.%C composite powders predicted by the W-H method decreased respectively to 3.317 nm and 3.066 nm after MA for 24 h.

Keywords: Mechanical alloying; W powder composites; Crystallite size; Lattice strain; W-H method and Gaussian rule

Introduction

Tungsten (W) based alloys are good candidates for high temperature applications because of its high melting point, thermal shock resistance, high elastic modulus, low thermal expansion coefficient and high temperature strength and stiffness[1,2]. Due to W high melting point its fabrication is extremely difficult. Recently, powder metallurgy (PM) is one of the most interesting methods for W powder production since there is a potential field of applications in aerospace, chemical, transportation, structural and automotive industries [3,4]. Mechanically alloying (MA) technique broadly used in PM processing for attaining a homogeneous distribution and fine grained matrix [3-7].

MA process give rises to uniform dispersion for the fine reinforcements and grain size of the matrix. Reinforcing of the ductile W matrix with hard particles such as carbides and oxides provides an improvement of physical and mechanical properties of composites [3-10]. There is no literature about powder characterization which reports on tungsten matrix composites reinforced with VC and TiC. One theoretical model was proposed in which amorphization was assumed to be realized through interstitial impurity formation during MA [6,11]. When the local distortions achieved some critical value, the long-range order of the lattice was destroyed and an amorphous phase formed. It was also shown that the minimum concentration of solute atoms needed to amorphize a binary alloy system by MA was extremely related to the atomic size ratio of the constituents [6,12]. Meantime, measurements of crystallite size and lattice strain is very important because of the phase constitution and transformation characteristics that critically dependent on them [6]. The contributions of crystallite size and internal strain to the broadening of XRD peaks can be calculated by using extrapolated W-H method and Gaussian rule [13,14].

The objectives of the present study are phase and morphological characterization of MA'd W composite powders and investigate the effects of mechanical alloying (MA) time and titanium carbide (TiC) content on the effective lattice parameter (a), crystallite size and

lattice strain and amorphization rate of the W-2wt.%VC-1wt.%C and W-2wt.%VC-2wt.%TiC-1wt.%C composite powders. Moreover, morphologies of powders after MA at various durations were studied and their specific surface areas were measured.

Materials and Experimental Procedure

Materials

Elemental tungsten (W) powders (Eurotungstene™, 99.9% purity, 17 μm) as the matrix of the powder composite and vanadium carbide (VC) powders (ABCRTM, 99.9% purity, 7 μm) and titanium carbide (TiC) powders (Alfa Aesar™, 99.9% purity, 15 μm) reinforcing particles were utilized in this investigation. Moreover, 1 wt% graphite powders (Alfa Aesar™, 99.9% purity, 21 μm) were added to each batch as a process control agent (PCA) to eliminate cold welding between powder particles and thereby to prevent agglomeration.

High energy ball milling

W, VC, TiC and C powders were blended to constitute the compositions of W-2wt.%VC-1wt.%C and W-2wt.%VC-2wt.%TiC-1wt.%C (thereafter referred to as W-2VC-1C and W-2VC-2TiC-1C) which were mechanically alloyed for 1, 3, 6, 12 and 24 h. High-energy milling experiments were carried out in a Spex™ DuoMixer/Mill 8000D using a tungsten carbide (WC) vial and WC balls (6.35 mm in diameter) as milling media. The ball-to-powder weight ratio (BPR)

*Corresponding author: Sonmez S, Istanbul Technical University, Department of Metallurgical and Mater Engineering, 34469, Istanbul/Türkiye, Tel: 0000-0003-1371-9869; E-mail: sultansonmez@itu.edu.tr

Received August 16, 2016; Accepted October 12, 2016; Published October 20, 2016

Citation: Sonmez S, Jahangiri H, Ovecoglu ML (2016) Effects of TiC Additions on Physical Properties of W-2wt.%VC-1wt.%C Nano Powder Composites Fabricated by Mechanical Alloying. J Powder Metall Min 5: 145. doi:10.4172/2168-9806.1000145

Copyright: © 2016 Sonmez S, et al. This is an open-access article distributed under the terms of the Creative Commons Attribution License, which permits unrestricted use, distribution, and reproduction in any medium, provided the original author and source are credited.

was 10:1. To avoid oxidation during MA, the vials were sealed inside a Plaslabs™ glove box under Ar gas (99.995% purity).

Morphological analysis

Morphological characterizations were carried out using the Jeol™ WX-36210DPP EDS unit (Energy Dispersive Spectrometer) with an accelerating voltage 15 kV. Particle distribution, size and morphologies were investigated by using SEM images. Powder particle size measurements were carried out in a Malvern™ Master-sizer Laser particle size analyzer. Furthermore, MA'd nano particle size distributions were measured by a Microtrac™ NANO-flex In-situ particle size analyzer.

Structural evolutions

X-ray diffraction (XRD) measurements were carried out in a Bruker™ X-Ray Diffractometer ($\lambda=1.5405\text{\AA}$) at 35 kV and 40 mA settings in the 2θ range from 30° to 110° at a scanning speed of 2° min^{-1} . To eliminate equipment effects, the LaB_6 crystal was used as a standard sample. The crystallite size and lattice strain were estimated using the Williamson–Hall method [15].

$$\beta_s + \cos \theta = \frac{K\lambda}{D} + 4\epsilon \sin \theta \quad (1)$$

where β_s is the full-width at half-maximum of the diffraction peak, θ is the diffraction angle, λ is the X-ray wavelength, D is the crystallite size and ϵ is the lattice strain and K is constant equal 0.9. β_s can be given as:

$$\beta_s^2 = \beta_e^2 - \beta_i^2 \quad (2)$$

Where β_s is the width at half-maximum of the LaB_6 powder peaks used for calibration and β_e is the width at half-maximum of the W. It is clear that when $\beta_s \cos \theta$ is plotted against $\sin \theta$, a straight line with slope (ϵ) and intercept $K\lambda/D$ is obtained [16]. Lattice parameters were determined by using three major diffraction peaks of tungsten $\{(110), (200) \text{ and } (211)\}$ in order to increase the precision of the measurements. Meanwhile, lattice strain and crystallite size were measured by Gaussian methods via TOPAS 3 (BRUKER AXS). Besides, the percent crystallinity were calculated by using EVA Bruker™ software.

Powder density and surface area measurement

Bulk densities of MA'd nano-sized powder composites were measured using a Micromeritics AccuPyc™ II 1340 helium pycnometer. The specific surface area of the nano powder composites was measured using a surface area analyzer (Quantachrome Instruments™ Autosorb-1 Series, Surface Area and Pore Size Analyzers). The specific surface area of nano powder composites was calculated by the Brunauer–Emmett–Teller (BET) method. Sample surface was first regenerated to remove the adsorbed gases and moisture by degassing in vacuum at 180°C . Specific surface area was calculated by measuring the volume of N_2 adsorbed using a modified multi point BET equation.

Results and Discussion

Morphology

Figure 1a-1f are representative SEM micrographs of MA'd W-2VC-1C and W-2VC-2TiC-1C nanocomposite powders milled at durations of 1 h, 6 h and 24 h, respectively. It is appointed that the particle size is changing with mechanical alloying time, because of the two opposing phenomena of cold welding and fracturing of powders [6]. 1 h milling, the powders exhibit large irregular shapes, see Figure 1a and 1d, and then were dramatically changed in particle sizes after 6

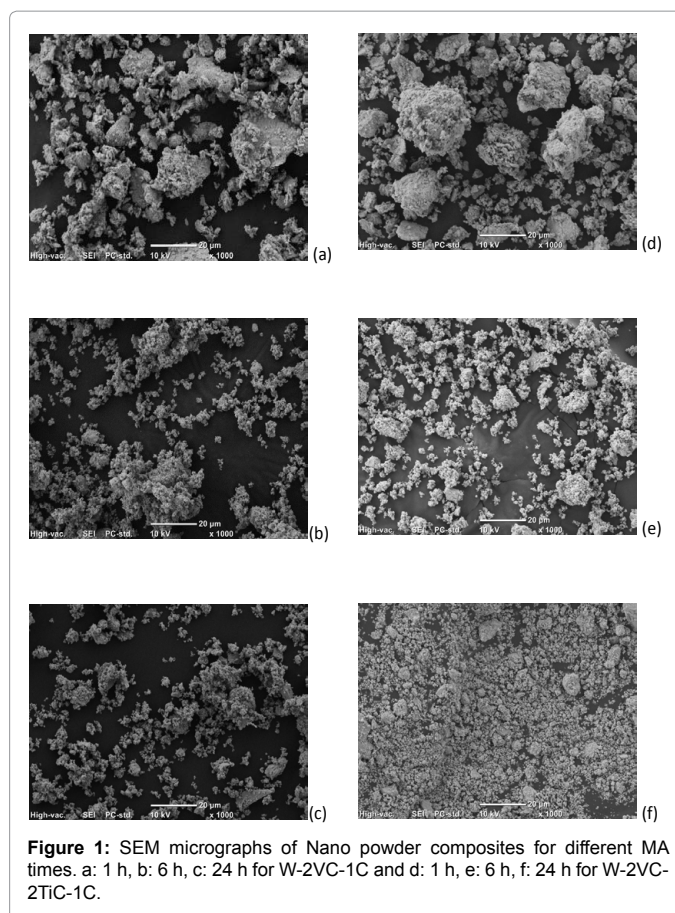


Figure 1: SEM micrographs of Nano powder composites for different MA times. a: 1 h, b: 6 h, c: 24 h for W-2VC-1C and d: 1 h, e: 6 h, f: 24 h for W-2VC-2TiC-1C.

h milling, as shown in Figure 1b and 1e. After 24 h MA time, more fine and homogeneous particle size distribution were shown in Figure 1c and 1f. It suggests that with continued plastic deformation the particles were hardened and fractured by fatigue failure or fragmentation [17]. MA'd W-2VC-2TiC-1C powders have some greater particles than W-2VC-1C at same MA durations. It means that, TiC declined particle size decreasing rate. This phenomena was approved by particle size distribution which measured in nano-sizer (Microtrac™ NANO-flex). It should be established that the mechanical alloying process not only refines the powder but also causes significant lattice strain and hence increases the dislocations in the powder crystals [18]. Such results are in agreement with those reported in different papers concerning the production of powders by high energy ball milling [6-9,19,20].

Structural analysis

X-ray diffraction patterns of W-2VC-1C and W-2VC-2TiC-1C powder composites for different milling times are shown in Figures 2 and 3. The XRD patterns of powders reveal the presence of the characteristic peaks of the W phase which has a b.c.c. Bravais lattice and $\text{Im}3m$ space group with the lattice parameter of $a=0.316 \text{ nm}$ [Powder Diffraction Files: Card No. 04-0806, database edition, The International Centre for Diffraction Data (ICDD)]. Only W peaks can be seen and characteristic peaks of VC, TiC and C do not appear because of their low amounts (Figures 2 and 3).

With increase in milling time, XRD peak intensities reduced drastically due to the reduction of powders particles to submicron sizes and/or the low volume fraction of the mechanically alloyed powders [21-23].

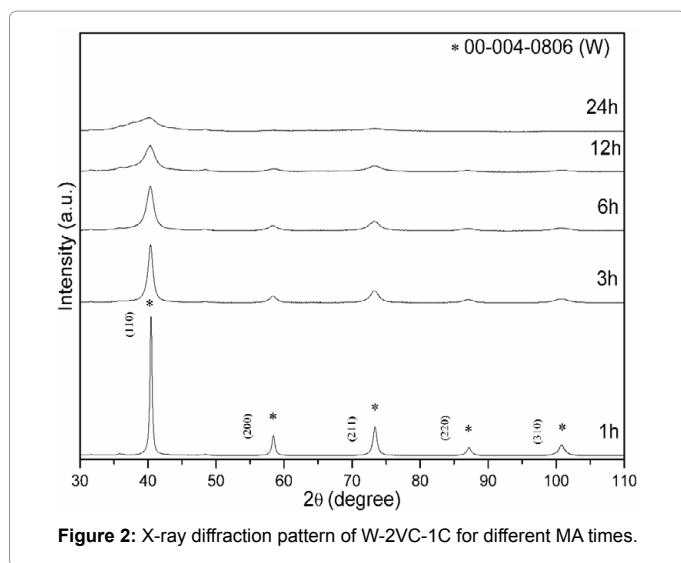


Figure 2: X-ray diffraction pattern of W-2VC-1C for different MA times.

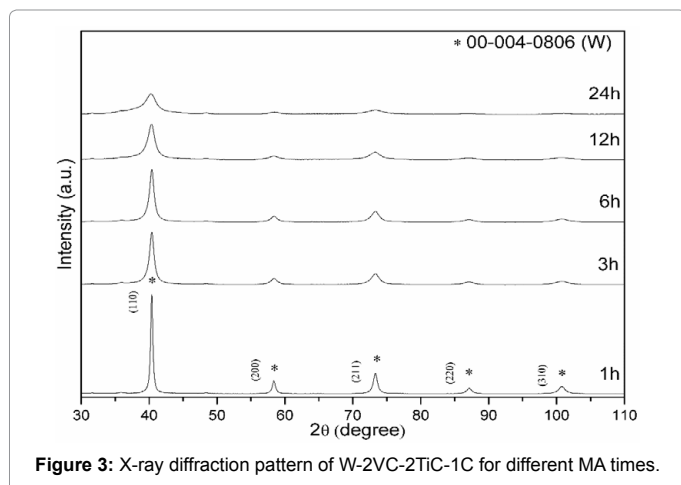


Figure 3: X-ray diffraction pattern of W-2VC-2TiC-1C for different MA times.

Figures 2 and 3 show the blow-up regions of XRD patterns in the vicinity of the major peak {110} of W at different milling times for the W-2VC-1C and W-2VC-2TiC-1C nanocomposites, respectively. That the W (110) peak shifts to lower angles with increasing milling time as shown in Figures 2 and 3 is a clear indication of increased C solubility in the W matrix and lattice internal strain induced by MA impaction [8]. Further increase in MA duration results in further broadening of the peaks of both phases as a result of grain refinement and build up strain during MA. Moreover, increasing the milling time leads to broadening of the W peaks and decreasing of their intensities, which demonstrate reduction in crystallite size and accumulation of strain in the materials [10,24].

The effect of milling time on the crystallite size and the strain of composite powders is illustrated in Figures 4 and 5. The lattice strains and the crystallite size of the powders were calculated by Gaussian and Williamson-Hall (W-H) methods. The crystallite sizes and the retained strain of the MA'd composite powders were measured by using TOPAS 3 (Bruker™ AXS) software with Gaussian techniques [25]. Also, Eq.1 was used to calculate these values from XRD data in W-H method. The peak broadening owing to the crystallite size and the lattice strain increases rapidly with increasing Θ , but the separation between these two values is clearer at smaller Θ . So, it is reasonable to utilize peaks

with smaller Θ to distinct these two effects [10,16]. Thus crystallite size and strain was determined using 3 small angle peaks {(110), (200) and (211)} in order to enhance the precision of the measurements.

The effect of milling time on the strain of composite powders is presented in Figure 4. As shown in this figure, internal lattice strain of W-2VC-1C and W-2VC-2TiC-1C calculated via W-H and Gaussian methods were increased by increasing MA time. Up to 6 h for W-2VC-1C and W-2VC-2TiC-1C powder compositions, the strain values (0.651 and 0.652 respectively) increase rapidly and from 6-24 h strain values (1.323 and 0.884 after 24 h respectively) enhancement occurs slowly in W-H method. While strain values obtained by Gaussian method approximately increased linearly. Crystal defects such as dislocations and point defects were increased via MA [16,26]. The formed defects increase internal lattice strain and energy so it becomes unstable. The dislocations rearrange themselves to a lower energy state leading to the formation of sub-grain. At longer times of milling and therefore, higher plastic deformation and generation of more dislocations, the misorientations between sub-grains at their boundaries increase and

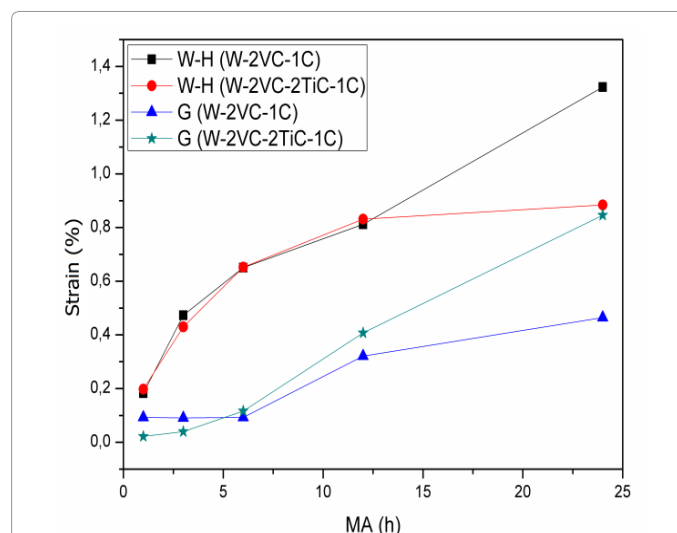


Figure 4: W-2VC-1C and W-2VC-2TiC-1C strain via different methods (Gaussian, Williamson-Hall) for different MA times.

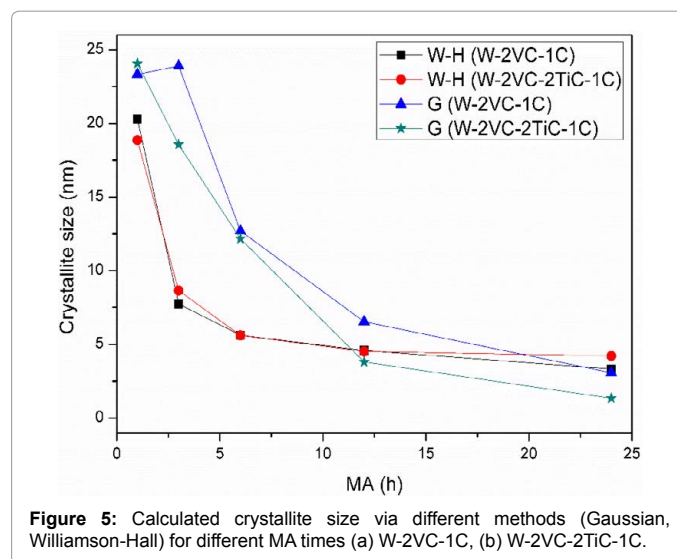


Figure 5: Calculated crystallite size via different methods (Gaussian, Williamson-Hall) for different MA times (a) W-2VC-1C, (b) W-2VC-2TiC-1C.

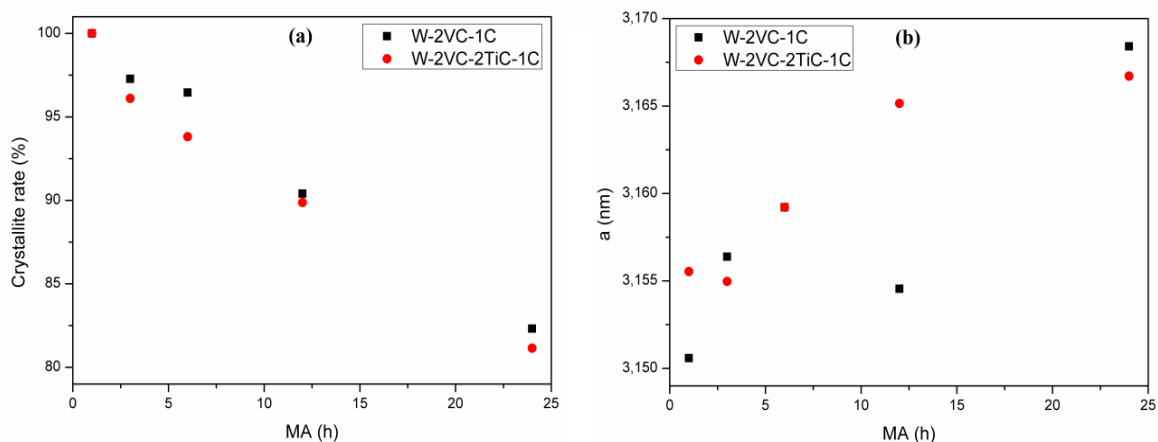


Figure 6: Variation of crystallite rate and lattice parameter as a parameter of MA time for W-2VC-2TiC-1C and W-2VC-1C nanocomposites.

finally, they convert to high angle boundaries and become grains with nano sizes [10,26,27].

Crystallite size variations of W-2VC-1C and W-2VC-2TiC-1C matrix versus MA time are offered in Figure 5. For W-2VC-1C and W-2VC-2TiC-1C compositions, up to 6 h, the crystallite size decreases rapidly (5.614 nm and 12.700 nm respectively) and then diminishes slowly (3.317 nm and 3.066 nm respectively for 24 h) in W-H method. Meantime, crystallite size amounts were measured by Gaussian method like W-H method.

In Figure 6a, crystallized rate and lattice parameter versus MA time for W-2VC-1C and W-2VC-2TiC-1C powder composites were illustrated. The crystallization rate of W-2VC-1C and W-2VC-2TiC-1C powder composites linearly decreased to 82% and 80% respectively MA time increment. TiC addition increased amorphization rate of the W-2VC-1C powder composites. During MA, destabilization of the crystalline phase is thought to occur by the accumulation of structural defects such as vacancies, dislocations, grain boundaries, and anti-phase boundaries. These defects raise the free energy of the system to a level higher than that of the amorphous phase and accordingly, it becomes possible for the amorphous phase to form [16]. These figures illustrate that (200), (220) and (310) peaks were disappeared after 24 h MA time. That approves amorphization rate increment by MA.

Figure 6b shows that “a” values increase by MA time increment. It means that, lattice parameter expanded and lattice interplaner distances increased. This fact relates XRD peaks slipping toward the lower angles due to MA period increment. As shown in Figure 6b with up to 24 h MA, lattice parameter (a) increases due to interstertion of C atoms into W lattice [6] and grain refinement [28,29]. This was inferred by the clear shift of the W peaks toward lower angles (Figures 2b and 3b).

Powder density and specific surface area

Powder theoretical densities of W-2VC-1C and W-2VC-2TiC-1C composites are 17.18 and 16.40 g/cm³ respectively, which decreased to 13.30 and 13.62 g/cm³ after 24 MA respectively. After 24 h MA duration, *d*₅₀ particle size measured as ~228 nm and ~174 nm for W-2VC-1C and W-2VC-2TiC-1C respectively. This is supported with SEM analysis in Figure 1c-1f, W-2VC-2TiC-1C powder composites have smaller particle size than W-2VC-1C, and similarly, after 24 h MA duration, specific surface areas values of W-2VC-2TiC-1C increase more than W-2VC-1C.

Conclusions

The morphological and structural changes of W-2VC-1C and W-2VC-2TiC-1C powder composites during mechanical alloying were studied. From this study the following conclusions could be drawn:

1. Mechanical alloying process not only refines the W-2VC-1C and W-2VC-2TiC-1C composite powder but also causes significant lattice strain and hence increases the dislocations in the powder crystals.

Addition of TiC declined particle size decreasing rate.

2. By solution of C atoms in the W matrix due to MA, the characteristic peaks of W shift toward lower angles.

3. Up to 6 h MA time for W-2VC-1C and W-2VC-2TiC-1C powder compositions, the strain values (0.651 and 0.652 respectively) increase rapidly and from 6-24 h strain values (1.323 and 0.884 after 24 h MA time respectively) enhancement occurs slowly in W-H method. While strain values obtained by Gaussian method approximately increased linearly.

4. For W-2VC-1C and W-2VC-2TiC-1C compositions, up to 6 h MA time, the crystallite size decreases rapidly (5.614 nm and 12.700 nm respectively) and then diminishes slowly (3.317 nm and 3.066 nm respectively for 24 h) in W-H method. Meantime, crystallite size values measured by Gaussian method like W-H method.

5. The crystallization rate of W-2VC-1C and W-2VC-2TiC-1C powder composites linearly decreased to 82% and 80% respectively after 24 h MA time. TiC addition increased amorphization rate of the W-2VC-1C powder composites.

6. The characteristic W peaks (200), (220) and (310) were disappeared after 24 h MA time.

7. In both compositions, lattice parameter expanded and lattice interplaner distances increased due to MA period increment.

8. After 24 MA time, powder densities decreased from 17.18 and 16.40 g/cm³ to 13.30 and 13.62 g/cm³ respectively.

Acknowledgements

This work was supported by the <Scientific and Research Projects Coordination Unit (BAP) of Istanbul Technical University> under Grant <number 39825>.

References

1. Lassner E, Schubert WD (1999) *Tungsten: Properties, chemistry, Technology of the element, Alloys and chemical compounds*. Kluwer Academic, NewYork.
2. Fang ZZ (2010) *Sintering of advanced materials fundamentals and processes*, Woodhead publishing 365-380.
3. Genç A, Coşkun S, Öveçoğlu ML (2010) Decarburization of TiC in Ni activated sintered W-xTiC (x=0, 5, 10, 15 wt%) composites and the effects of heat treatment on the microstructural and physical properties. *International Journal of Refractory Metals and Hard Materials* 28(3): 451-458.
4. Ağaoğulları D, Balci Ö, Demirkan ÖU, Gökçe H, Genç A, et al. (2013) Development of mechanically alloyed and sintered W-1wt% Ni Matrix composites Reinforced with TiB₂. *solid state phenomena* 194-198.
5. Lu L, Zhang YF (1999) Influence of process control agent on interdiffusion between Al and Mg during mechanical alloying. *Journal of Alloys and Compounds* 290.1: 279-283.
6. Suryanarayana C (2001) Mechanical alloying and milling. *Progress in materials science* 46.1: 1-184.
7. Gubicza J, Kassem M, Ribárik G, Ungár T (2004) The microstructure of mechanically alloyed Al-Mg determined by X-ray diffraction peak profile analysis. *Materials Science and Engineering A* 372.1: 115-122.
8. Wagih A (2015) Mechanical properties of Al-Mg/Al₂O₃ nanocomposite powder produced by mechanical alloying. *Advanced Powder Technology* 26.1: 253-258.
9. Fathy A, Wagih A, El-Hamid MA, Hassan AA (2014) The effect of Mg add on morphology and mechanical properties of Al-xMg/10Al₂O₃ nanocomposite produced by mechanical alloying. *Advanced Powder Technology* 25.4.
10. Safari J, Akbari GH, Shahbazkhan A, Chermahini MD (2011) Microstructural and mechanical properties of Al-Mg/Al₂O₃ nanocomposite prepared by mechanical alloying. *Journal of Alloys and Compounds* 509.39: 9419-9424.
11. Chakk Y, Berger S, Weiss BZ, Brook-Levinson E (1994) Solid state amorphization by mechanical alloying—an atomistic model. *Acta metallurgica et materialia* 42(11): 3679-3685.
12. Egami T (1984) Magnetic amorphous alloys. physics and technological applications. *Reports on Progress in Physics* 47(12): 1601.
13. Lubarda V (2003) On the effective lattice parameter of binary alloys. *Mechanics of Materials* 35(1-2): 53-68.
14. Williamson GK, Hall WH (1953) X-ray line broadening from filed aluminum and wolfram. *Act Metal* 1(1): 22-31.
15. Hall WH, Williamson GK (1951) The diffraction pattern of cold worked metals: I the nature of extinction. *Proceedings of the Physical Society. Section B* 64.11: 937.
16. Suryanarayana C, Norton MG (1998) X-ray diffraction: a practical approach. *Microsc Microanal* 4: 513-5.
17. Chen CL, Chun LH (2013) The effects of alloying and milling on the formation of intermetallics in ODS tungsten heavy alloys. *Intermetallics* 41: 10-15.
18. Chen CL, Dong YM (2011) Effect of mechanical alloying and consolidation process on microstructure and hardness of nanostructured Fe-Cr-Al ODS alloys. *Materials Science and Engineering A* 528.29: 8374-8380.
19. Furlani E, Aneggi E, de Leitenburg C, Maschio S (2014) High energy ball milling of titania and titania-ceria powder mixtures. *Powder Technology* 254: 591-596.
20. Dodd AC, McCormick PG (2003) Factors affecting the particle size of powders synthesised by mechanochemical processing. *Journal of Metastable and Nanocrystalline Materials* 15.
21. Zhao L, Jochen Z, Erich L (2003) The influence of milling parameters on the properties of the milled powders and the resultant coatings. *Surface and Coatings technology* 168.2: 179-185.
22. Demirkan ÖU, Genç A, Öveçoğlu ML (2012) Effects of Al₂O₃ addition on the microstructure and properties of Ni activated sintered W matrix composites. *International Journal of Refractory Metals and Hard Materials* 32: 33-38.
23. Genç A, Öveçoğlu ML (2010) Characterization investigations during mechanical alloying and sintering of Ni-W solid solution alloys dispersed with WC and Y₂O₃ particles. *Journal of Alloys and Compounds* 508.1: 162-171.
24. Sivasankaran S, Sivaprasad K, Narayanasamy R, Satyanarayana PV (2011) X-ray peak broadening analysis of AA6061 100-x-xwt.%Al₂O₃ nanocomposite prepared by mechanical alloying. *Materials characterization* 62.7: 661-672.
25. Bruker AXS (2005) TOPAS V3: General profile and structure analysis software for powder diffraction data. User's Manual, Bruker AXS, Karlsruhe, Germany.
26. Saberi Y, Zebarjad SM, Akbari GH (2009) On the role of nano-size SiC on lattice strain and grain size of Al/SiC nanocomposite. *Journal of Alloys and Compounds* 484.1: 637-640.
27. Zhang FL, Wang CY, Zhu M (2003) Nanostructured WC/Co composite powder prepared by high energy ball milling. *Scripta materialia* b 49.11: 1123-1128.
28. Chermahini MD, Zandrahimi M, Shokrollahi H, Sharafi S (2009) The effect of milling time and composition on microstructural and magnetic properties of nanostructured Fe-Co alloys. *Journal of Alloys and Compounds* 477.1: 45-50.
29. Chermahini MD, Sharafi S, Shokrollahi H, Zandrahimi M (2009) Microstructural and magnetic properties of nanostructured Fe and Fe 50 Co 50 powders prepared by mechanical alloying. *Journal of Alloys and Compounds* 474.1: 18-22.

Citation: Sonmez S, Jahangiri H, Ovecoglu ML (2016) Effects of TiC Additions on Physical Properties of W-2wt.%VC-1wt.%C Nano Powder Composites Fabricated by Mechanical Alloying. *J Powder Metall Min* 5: 145. doi:10.4172/2168-9806.1000145

OMICS International: Open Access Publication Benefits & Features

Unique features:

- Increased global visibility of articles through worldwide distribution and indexing
- Showcasing recent research output in a timely and updated manner
- Special issues on the current trends of scientific research

Special features:

- 700+ Open Access Journals
- 50,000+ editorial team
- Rapid review process
- Quality and quick editorial, review and publication processing
- Indexing at major indexing services
- Sharing Option: Social Networking Enabled
- Authors, Reviewers and Editors rewarded with online Scientific Credits
- Better discount for your subsequent articles

Submit your manuscript at: <http://www.omicsonline.org/submission>